Available online at www.sciencedirect.com

ScienceDirect

Mendeleev Commun., 2020, **30**, 282–284

Mendeleev Communications

In situ growth of four MOF/LZH composites on layered zinc hydroxide and their photocatalytic performance in decomposition of organic dyes

Jiehu Cui,*[a] Ming Zhang,[a] Chunlei Wei,[a] Jie Zhu,[a] Xiangping Wang[a] and Xiuhong Du[b]

[a] *Zhengzhou University of Aeronautics, 450015 Zhengzhou, P. R. China. E-mail: cuijiehu@163.com*
[b] *Henan Medical College, 451191 Zhengzhou, P. R. China.*

DOI: 10.1016/j.mencom.2020.05.006

Four new MOF/layered zinc hydroxide composites suitable for photocatalytic decomposition of organic dyes were prepared *via* an *in situ* growth on layered zinc hydroxide according to the solvothermal procedure and characterized by SEM, XRD, IR spectroscopy, and N_2-adsorption/desorption. All the selected pollutant dyes (methyl orange, congo red, brilliant green, sunset yellow, and amaranth) underwent a very efficient photodegradation by MOF/LZH-6 composite upon the UV irradiation (λ = 365 nm) *via* their oxidation by OH radicals and super oxide anion radical species.

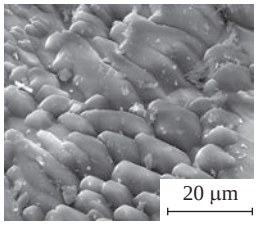

Keywords: MOF/LZH composites, layered zinc hydroxide, photocatalytic decomposition, organic dyes, wastewater treatment.

Metal-organic frameworks (MOFs) as a novel class of crystalline hybrid materials possessing the unique highly ordered porous structure are gaining widespread scientific attention due to their potential applications in luminescence sensing, chemical sensors, separation of substances, catalysis, *etc.*[1] MOFs are of especial interest as promising heterogeneous catalysts.[2] The heterogeneous photocatalysts such as TiO_2, ZnO, Fe_2O_3, and ZnS have already been demonstrated as highly efficient in the degradation of organic pollutants,[3–6] but the photostability of these photocatalysts was low under the operating conditions. Thus, it is important to look for new photocatalysts with an improved performance. Recent reports have revealed that some MOFs are potentially useful as the photocatalysts due to the diversities of metal-organic ligand charge transfer.[7–9] MOF-5 as a photocatalyst was firstly applied owing to its broad absorption band ranging from 500 to 840 nm.[10]

Organic dyes hardly undergo a biodegradation because of their high concentrations, deep colours, and high stability under conditions of the conventional biological method for a wastewater treatment.[11] Among some methods for dye removal such as adsorption, photocatalysis, membrane filtration, and oxidation,[12–14] the photocatalytic technologies are favourable due to their economic feasibility, simplicity of implementation, and nonexistence of any harmful residues.

Inspired by a MOF-5 application for the photocatalytic decomposition of pollutants and Zn/Al/CO_3 layered double hydroxide (LDH) as a Zn precursor for the synthesis of MOFs,[15] we have designed a layered Zn hydroxide (LZH) salt materials *via* a facile hydrothermal technology in the presence of triethanolamine.† At the best of our knowledge, there are no systematic studies on LZH as a Zn-containing precursor for the preparation of MOF/LZH composite. In the present work, four MOF (MOF-69A)/LZH composites have been successfully prepared *via* a solvothermal procedure at 120 °C (within 2, 4, 6 and 8 h), which is the modification of reported hydrothermal method (at 95 °C for 72 h in an oven),[16] and designated herein as MOF/LZH-2, MOF/LZH-4, MOF/LZH-6, and MOF/LZH-8, respectively.‡

Based on comparison of the as-synthesized LZH (ICDD 24-1460) with lamellar and quadrilateral ones,§,[17] it was found that MOF/LZH-2 composite has been successfully produced *via* the nucleation and growth of MOF-69A on the LZH surface within 2 h using LZH as the Zn precursor [Figure 1(*a*)]. Figure 1(*b*) shows that there is an additional amount of MOF grown on the LZH

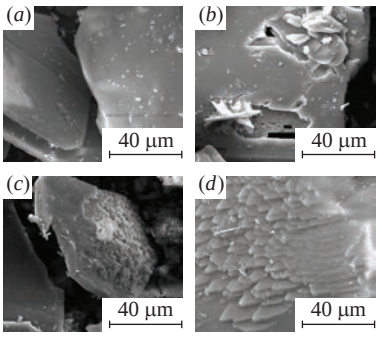

Figure 1 SEM images of MOF/LZH obtained within: (*a*) 2, (*b*) 4, (*c*) 6 and (*d*) 8 h.

† All the used reagents and solvents were purchased from commercial sources and used as received.

‡ *General procedure*. MOF/LZH composites were synthesized using LZH as the source of Zn^{2+} according to the modified solvothermal method.[16] The prepared LZH (5 mmol) was dispersed in a DMF/H_2O (deionized) mixure (25 ml, 1:2, v/v) and stirred for 5 min. Then, biphenyl-4,4′-dicarboxylic acid (5 mmol) was slowly added under stirring. The resulting mixture was placed in a Teflon-lined stainless steel vessel and kept in an oven at 120 °C for 2 h. After that, it was cooled down to room temperature, solid products at the bottom of autoclave were washed with deionized water several times and dried at 60 °C for 24 h. A series of MOF/LZH composite photocatalysts was obtained *via* a variation of the synthesis time (2, 4, 6 and 8 h).

§ See Online Supplementary Materials for the related details.

© 2020 Mendeleev Communications. Published by ELSEVIER B.V. on behalf of the N. D. Zelinsky Institute of Organic Chemistry of the Russian Academy of Sciences.

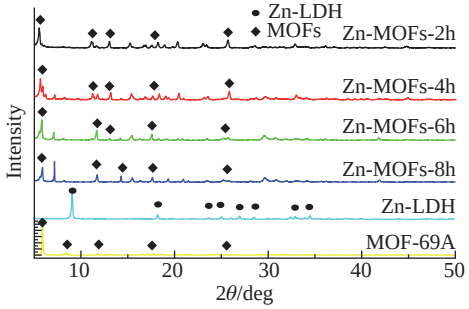

Figure 2 XRD patterns of four MOF/LZH composites in comparison with MOF-69A and LZH. Peaks marked with rhombuses and dots represent diffraction peaks from MOF layer and LZH network, respectively.

surface during 4 h. Upon increasing the duration of synthesis, more and more portions of MOF-69A are being grown on the LZH surface, a flat surface is becoming rough with the formation of cracks, bulges, and crumbling points within 6 h [Figure 1(*c*)]. Finally, a regular appearance has been formed on the LZH surface within 8 h [Figure 1(*d*)]. These findings show an important role of time in the preparation of MOF/LZH composites, the MOF mass increasing upon the prolongation of reaction time. So, this route can be used as a convenient way to synthesize the MOF/LZH composites through tuning the duration of reaction.

Figure 2 shows XRD patterns of the obtained MOF/LZH composites. According to the known crystal structure data on MOFs (CCDC 1431701),[16] the acquired XRD results for our MOF/LZH composite are in a good agreement with the simulated XRD pattern of MOFs possessing an orthorhombic space group (*Pnnm*). At the same time, we have also found that the peaks at 200 of LZH disappeared, which confirmed that this reaction proceeded at the 200 crystal plane of LZH, and this phenomenon was also in a good agreement with SEM data. Thus, LZH is a desirable and versatile precursor for the heterogeneous nucleation of MOF/LZH composite. New methods for the preparation of MOFs are still a crucial challenge, and they are based on various metal sources, such as metal oxides, hydroxides, and acetates.[18,19] In the present work, this route can be used as an alternative option for the *in situ* synthesis of MOFs, based on LZH as the Zn^{2+} precursor.

The XRD data (see Figure 2) have also revealed changes in the composition and structure of the MOF/LZH upon variations in the reaction time. As the time increases, the diffraction and intense peaks of MOF become more obvious. Comparing to the diffraction and intense peaks of pure LZH and MOF, the peak of MOF/LZH at 9.21° has disappeared, while MOF peaks have arisen at 5.82, 7.28, 11.58 and 15.46°, which suggests proceeding of the nucleation reaction over 200 crystal plane and confirms the successful formation of MOF/LZH layer.

The surface area and pore size distribution of four MOF/LZH composites was investigated by N_2 adsorption–desorption measurements. The isotherm for this process and the corresponding pore size distribution for the MOF/LZH composites were plotted (Figure S2, see Online Supplementary Materials). Obviously, this isotherm is consistent with a type IV of adsorption isotherms containing an H3-type hysteresis without any limiting adsorption at high P/P_0 loop according to the IUPAC classification.

The determined BET surface areas of MOF/LZH-2, MOF/LZH-4, MOF/LZH-6 and MOF/LZH-8 composites were 3.48, 3.10, 3.82 and 3.02 $m^2\ g^{-1}$, and the pore volume was 0.01209, 0.008066, 0.01198 and 0.01166 $cm^3\ g^{-1}$, respectively. A comparison with the values of BET surface area and pore volume (18.15 $m^2\ g^{-1}$ and 0.1099 $cm^3\ g^{-1}$) for pure LZH indicates that the corresponding values of all the samples are low, which may be associated with the crowded and compact composite layers in the case of MOF/LZH rather than lamellar and quadrilateral ones for the layer of pure LZH. The pore sizes of the four obtained MOF/LZH composites were 14.85, 11.44, 13.15 and 15.71 nm, so each of these values is smaller than that (24.22 nm) of pure LZH. This implies that mesopores and macropores are coexistent in all the MOF/LZH composites reported here.

Furthermore, the considered MOF/LZH composites were characterized by FTIR spectroscopy (Figure S3). A vibration band at 3436 cm^{-1} indicates the presence of OH group of water molecules. The presence of sharp band at 1383 cm^{-1} was assigned to the asymmetric vibration of nitrate, which is similar to that of pure LZH, thus demonstrating a preservation of the layered structure in MOF/LZH-2, MOF/LZH-4, MOF/LZH-6 and MOF/LZH-8 composites. Skeletal vibrations of the aromatic rings were observed in the region of 1400–1600 cm^{-1}, which indicates that MOF/LZH-2, MOF/LZH-4, MOF/LZH-6 and MOF/LZH-8 composites are different.

A comparison of solid UV-VIS spectra of LZH recorded in the interval from 200 to 240 nm (Figure S4) with the corresponding solid UV-VIS spectra of four MOF/LZH composites (Figure S5) shows the strong absorption and red shift from 220 to 400 nm in the latter case. The absorption band edge of all the MOF/LZH composites was around 400 nm. At the same time, there was no any obvious variation in the UV-VIS diffuse reflectance spectra (DRS) for the different MOF/LZH composites. Comparison with the absorption band edge at 240 nm of LZH indicates that the MOF/LZH composites can be selected as potential photocatalysts. The band gap energy can be determined using UV-VIS DRS according to the Kubelka–Munk equation. The E_g values of four MOF/LZH composites (–2, –4, –6 and –8 ones) were 3.22, 3.20, 3.22 and 3.21 eV, respectively, and correspond to that of ZnAlTi mixed metal oxides. Therefore, the obtained MOF/LZH composites should demonstrate a charge separation of the low energy, thus providing a higher photocatalytic activity than that of LZH (3.7 eV).[20]

It is generally known that the effect of recombination rate of photogenerated electron and holes is an important factor for the photocatalytic efficiency.[21] Thereupon, photoluminescence (PL) spectra were recorded for our MOF/LZH composites. In general, a lower PL intensity suggests the higher efficiency of charge transmission and lower electrons/holes recombination, which can improve the photocatalytic activity. The PL intensity of MOF/LZH-6 was the highest one, which seems to be inconsistent with above data. This may be explained by a large MOF quantity in MOF/LZH-6 composite, which can increase the absolute amount of photogenerated carriers to a greater extent than the electrons/holes recombination through the UV absorption.

Currently, organic dyes are among major pollutants that are difficult to be degraded.[22] To investigate the photocatalytic ability of obtained MOF/LZH composites, we have investigated their photodegradation performance using methyl orange dye as the example of a pollutant. Figure 3 shows the photodegradation effect caused by the MOF/LZH composites. The MOF/LZH-6 has exhibited the best photocatalytic activity. At the same time, to determine whether methyl orange can be directly photolyzed upon

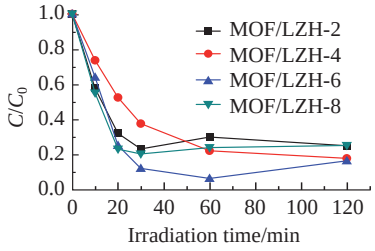

Figure 3 Photocatalytic degradation of methyl orange caused by the MOF/LZH composites.

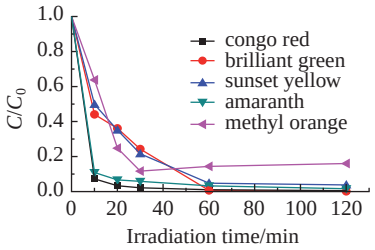

Figure 4 Photocatalytic degradation of methyl orange, congo red, brilliant green, sunset yellow, and amaranth, catalyzed by MOF/LZH-6.

the UV irradiation, a blank experiment was conducted without any catalyst. Its result has confirmed that the photodegradation of methyl orange without any catalyst also proceeds under UV irradiation (λ = 365 nm). However, its photodegradation is sharply increased in the presence of considered MOF/LZH composites within the first 30 min effecting the following order: MOF/LZH-6 > MOF/LZH-8 > MOF/LZH-2 > MOF/LZH-4. Thus, MOF/LZH-6 was selected to investigate the photodegradation performance for the other considered pollutant dyes.

The set consisting of methyl orange, congo red, brilliant green, sunset yellow and amaranth dyes was examined at pH 7.0 in order to estimate the photocatalytic ability of MOF/LZH-6 (Figure 4). Within the first 30 min, all the target pollutant dyes were very efficiently degraded by MOF/LZH-6 composite upon UV irradiation (λ = 365 nm) at the following degradation rate: congo red > amaranth > methyl orange > brilliant green > sunset yellow. Then, the photodegradation of methyl orange has slowly reached equilibrium at the prolongation of time, so methyl orange was selected for the systematic investigation of photodegradation effect caused by MOF/LZH-6 composite.

The initial methyl orange concentration was the key factor in these investigations. The photocatalytic effect was estimated through varying the initial dye concentration from 10 to 50 mg dm^{-3} while keeping the amount of MOF/LZH-6, reaction temperature, and pH value constant. Figure 5 shows that the photocatalytic capacity increases upon a decrease of the methyl orange concentration. This can be explained by the fact that the catalytic sites reach their saturation upon the increase of initial dye concentration, so catalytic capability exists at its minimum value, while the initial methyl orange concentration has its maximum value. As a result, the initial dye concentration can be specified as 10 mg dm^{-3} for the best photocatalytic activity in this experiment with MOF/LZH-6 as a catalyst.

The acquired results demonstrate that all the examined pollutant dyes can be very efficiently degraded by MOF/LZH-6 composite upon the UV irradiation (λ = 365 nm). The probable reason is that the electrons produced by MOF/LZH-6 composite easily react with O_2 to generate super oxide anion radical species (Figure S12). Moreover, OH radicals appeared due to a reaction between holes in the valance band with H_2O molecules were also observed (Figure S13).[23] Thus, both the OH radicals and super oxide anion radical species are responsible for the oxidation of organic dyes.

In summary, the *in situ* growth of four new MOF/LZH composites for photocatalytic decomposition of organic dyes was successfully carried out by the hydrothermal technique using LZH as the Zn-containing precursor. SEM, XRD, IR and BET surface area data were acquired for these composites. Within the first 30 min, all the selected pollutant dyes underwent a very efficient degradation by MOF/LZH-6 composite upon UV irradiation (λ = 365 nm), revealing that a large quantity of MOF in MOF/LZH-6 composite can significantly increase the absolute amount of photogenerated carriers rather than the electrons/holes recombination through the UV absorption. The degradation rate for methyl orange is affected by the selection of particular MOF/LZH composite and initial dye concentration. The photocatalytic capacity increases upon a decrease of the given methyl orange concentration range. The catalytic sites reach their saturation with the increase in the initial concentration of methyl orange. Therefore, MOF/LZH-6 composite reported is a very promising photocatalyst for practical degradation of methyl orange in the process of wastewater treatment.

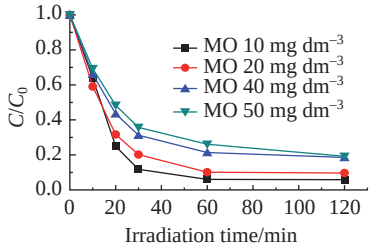

Figure 5 Photocatalytic degradation of methyl orange at its different concentrations, catalyzed by MOF/LZH-6 composite.

This work was supported by the National Natural Science Foundation of China (grant no. 21771165), the Key Program for the Henan Universities and Colleges (program no. 20B150031), and the Provincial Key Technologies R&D Programs of the Henan (program nos. 192102310237 and 172102310556).

Online Supplementary Materials

Supplementary data associated with this article can be found in the online version at doi: 10.1016/j.mencom.2020.05.006.

References

1 Y. Liu, N. Wang, L. Diestel, F. Steinbach and J. Caro, *Chem. Commun.*, 2014, **50**, 4225.
2 C.-C. Wang, J.-R. Li, X.-L. Lv, Y.-Q. Zhang and G. Guo, *Energy Environ. Sci.*, 2014, **7**, 2831.
3 M. V. Korolenko, P. B. Fabritchnyi, M. I. Afanasov and C. Labrugère, *Mendeleev Commun.*, 2019, **29**, 718.
4 M. I. Litter, *Appl. Catal., B*, 1999, **23**, 89.
5 U. G. Akpan and B. H. Hameed, *J. Hazard. Mater.*, 2009, **170**, 520.
6 K. Ayoub, E. D. van Hullebusch, M. Cassir and A. Bermond, *J. Hazard. Mater.*, 2010, **178**, 10.
7 F. X. Llabrés i Xamena, A. Corma and H. Garcia, *J. Phys. Chem. C*, 2007, **111**, 80.
8 Y. Horiuchi, T. Toyao, M. Takeuchi, M. Matsuoka and M. Anpo, *Phys. Chem. Chem. Phys.*, 2013, **15**, 13243.
9 M. A. Nasalevich, M. van der Veen, F. Kapteijn and J. Gascon, *CrystEngComm*, 2014, **16**, 4919.
10 M. Alvaro, E. Carbonell, B. Ferrer, F. X. Llabrés i Xamena and H. Garcia, *Chem. – Eur. J.*, 2007, **13**, 5106.
11 X. Guo, P. Yin and H. Yang, *Microporous Mesoporous Mater.*, 2018, **259**, 123.
12 S. Jauhar, S. Singhal and M. Dhiman, *Appl. Catal., A*, 2014, **486**, 210.
13 G. Huang, Y. Sun, C. Zhao, Y. Zhao, Z. Song, J. Chen, S. Ma, J. Du and Z. Yin, *J. Colloid Interface Sci.*, 2017, **494**, 215.
14 A. Roy, B. Adhikari and S. B. Majumder, *Ind. Eng. Chem. Res.*, 2013, **52**, 6502.
15 Y. Liu, N. Wang, J. H. Pan, F. Steinbach and J. Caro, *J. Am. Chem. Soc.*, 2014, **136**, 14353.
16 B. Fernández, G. Beobide, I. Sánchez, F. Carrasco-Marín, J. M. Seco, A. J. Calahorro, J. Cepeda and A. Rodríguez-Diéguez, *CrystEngComm*, 2016, **18**, 1282.
17 W. Stählin and H. R. Oswald, *J. Solid State Chem.*, 1971, **3**, 252.
18 G. Majano and J. Pérez-Ramírez, *Adv. Mater.*, 2013, **25**, 1052.
19 N. Stock and S. Biswas, *Chem. Rev.*, 2011, **112**, 933.
20 X. Wang, P. Wu, Z. Huang, N. Zhu, J. Wu, P. Li and Z. Dang, *Appl. Clay Sci.*, 2014, **95**, 95.
21 L. Ge and C. Han, *Appl. Catal., B*, 2012, **117**, 268.
22 A. A. Ulyankina, A. B. Kuriganova and N. V. Smirnova, *Mendeleev Commun.*, 2019, **29**, 215.
23 P. V. Pimpliskar, S. C. Motekar, G. G. Umarji, W. Lee and S. S. Arbuj, *Photochem. Photobiol. Sci.*, 2019, **18**, 1503.

Received: 18th November 2019; Com. 19/6058